

Fast photometry with small telescopes

G. Kanbach¹, A. Rau¹ and A. Słowikowska²

¹ *Max-Planck-Institute for extraterrestrial Physics, Giessenbachstrasse, 85748 Garching, Germany*

² *Kepler Institute of Astronomy, University of Zielona Góra, Lubuska 2, 65-265 Zielona Góra, Poland*

Received: November 15, 2013; Accepted: February 18, 2014

Abstract. Facility instruments on major telescopes rarely provide photometry on timescales into the sub-second range. The development of dedicated high-time resolution detectors that could be attached as guest instruments was therefore natural to follow up with optical observations on many highly time variable astronomical objects. Such sources were often discovered first in the radio range (e.g. pulsars, quasars) or with X- and gamma-ray satellites (X-ray binaries, cataclysmic variables, gamma-ray bursts). Although telescopes in the 4 - 8m class would be nice to have for high-time resolution astronomy (HTRA) the access is often oversubscribed. Many currently active HTRA instruments were started on smaller telescopes in the 1-3m class, which provide the flexibility and observation time needed for the observation of highly variable stars. We describe the basic detector types, i.e. fast imaging or photon counting, and current projects. Based on our experience with the fast timing photo-polarimeter OPTIMA (Optical Timing Analyzer), we review some observational constraints on meter-class telescopes. We demonstrate the 'scientific power' of very fast photometry, done with OPTIMA and similar systems on small telescopes, with selected results for a black hole binary, an optical transient magnetar, and the Crab pulsar.

Key words: high time resolution astronomy – photon counting detectors – OPTIMA – XTE J118+480 – SWIFT J195509.6+261406 – Crab

1. Introduction

The photon flux from a faint astronomical source, focussed on a detector mounted on a meter-class telescope, is statistically limited and has to be measured on top of the diffuse brightness of the night sky and the dark noise of a detector. Four points are therefore essential for a sensitive, fast photometer: (i) a broadband detector with high quantum efficiency to achieve the best counting statistics, (ii) accurate timing for either short CCD integration times or, preferably, time tagging for single detected photons, (iii) reliable distinction between source and the background, and (iv) continuous monitoring of the sky background and atmospheric conditions in order to control systematic errors.

2. Methods and Statistics

Fast photometry with small telescopes is critically dependent on the statistics available from (often faint) sources embedded in the background brightness of the night sky. In order to get a coarse estimate of this statistics and the signal to noise ratio in real observations we assume a source of average magnitude m_{src} and a sky brightness of $m_{sky}/arcsec^2$ and scale the count rate from observations of reference sources to obtain the calibration of optics and detector efficiency. The detection rate C_{src} for a source with magnitude m_{src} on a telescope with area A can be scaled from a reference rate C_o at magnitude m_o using a telescope with collecting area A_o :

$$C_{src} = C_o A 10^{b(m_o - m_{src})} / A_o \quad (1)$$

where C_o and b are calibration constants for a given setup; b should ideally be 0.4 but it is advisable to calibrate this constant with a sequence of reference stars of different magnitude. The sky background under and around the source is determined differently in systems that afford a full or partial 2-D resolution (CCD imager or integral field unit (IFU) of apertures) or single apertures. In the first type of camera, classical methods of photometry, i.e. fitting the source image on a flat background and relating it to catalogued stars in the field, are used. Seeing and background variations and telescope guider movements can be corrected well in CCD images. For a small IFU the count rate in the target aperture can also be corrected using the neighboring apertures with sky background rates. However one has to take care that aperture losses due to seeing or pointing errors might affect the rates from the apertures. In a system with a single aperture one might have to take extra on-source / off-source exposures to control the background. The estimate of a background rate depends on the angular resolution/pixel size and field of view of the detector system and on the plate scale provided by the telescope. The plate scale P , in units of $\mu m''$, is given by:

$$P = f \tan(1'') 10^6 = D f_{ratio} \tan(1'') 10^6 = 4.848 D f_{ratio} [\mu m''] \quad (2)$$

where f is the focal length, D is the prime mirror diameter (both in m) and the $f_{ratio} = f/D$. Usually CCD pixels are small with respect to the seeing disk image of a star and the background can be determined with good statistical accuracy in a large area around the target object. This is different for a system with fixed apertures. The sky inside an aperture with diameter $a [\mu m]$ subtends a sky area of $A_{bg} = 0.25\pi(a/P)^2 [']^2$ and the equivalent magnitude inside the aperture is then

$$m_{eq} = m_{sky} - 2.5 \log(\pi(a/2P)^2) = m_{sky} - 2.5 \log(\pi(a/9.696 D f_{ratio})^2) \quad (3)$$

The corresponding sky background rate is then

$$C_{sky} = C_o A 10^{b(m_o - m_{eq})} / A_o \quad (4)$$

It is evident that the sky background is reduced for small apertures (in units of the plate scale). The limiting size is however reached if the seeing leads to light loss. Reasonable apertures should be $\sim 6''$ in diameter to cover the variable seeing conditions at a good site.

If only one sky background measurement is available the error is $\Delta_{sky} = \sqrt{C_{sky}}$. For multiple measurements $C_{sky,i}$ the average background is

$$\langle C_{sky} \rangle = \frac{1}{N} \sum_{i=1}^N C_{sky,i} \quad (5)$$

and the error is

$$\Delta_{sky} = \sqrt{\frac{\sum_{i=1}^N (C_{sky,i} - \langle C_{sky} \rangle)^2}{N(N-1)}} \quad (6)$$

An estimate for the signal to noise ratio is:

$$\log(C_{src}/\langle C_{sky} \rangle) = -b[m_{src} - m_{sky} + 5 \log(\pi(a/9.696Df_{ratio})^2)] \quad (7)$$

The faintest detectable source and the minimal variation in the source flux can then be estimated from these equations.

As an example for realistic source rates, sky background rates, and limiting sensitivities we scale the calibration of the OPTIMA detector (Kanbach et al., 2003, 2008), which was obtained at the Skinakas Observatory (1.3 m mirror, University of Crete, Heraklion), to mirror sizes of 0.5, 1, and 2 m. The OPTIMA calibration was characterized by parameters (eqn. 1) of $C_o = 5140$ cps, $b = 0.389$, and $m_o = 13$ for the 1.3 m primary mirror aperture with an effective area $A_o = 1.15$ m². Figure 1 shows the scaled empirical rates under the assumption that aperture photometry is performed through a 300 μ m diaphragm, the f-ratio of the telescope is in the range f/8 to f/10, and the night sky brightness is 21 mag/arcsec². Tuning the aperture to the f-ratio of the telescope, choosing dark nights, and using multiple sky background measurements, can improve the sensitivity of the measurements.

3. Fast timing techniques and currently operating photometers

The term High Time Resolution Astronomy (HTRA) is mostly used for the observation of astrophysical phenomena that show variability with time scales in the range of seconds to nanoseconds. The development of new detectors with fast electronic readout systems, especially in the fields of radioastronomy and high-energy astronomy (X- and gamma-ray astronomy) enabled since the mid 20th century the discovery of extremely variable celestial objects. Active galactic nuclei, pulsars, gamma-ray bursts, and binary stars hosting white dwarves,

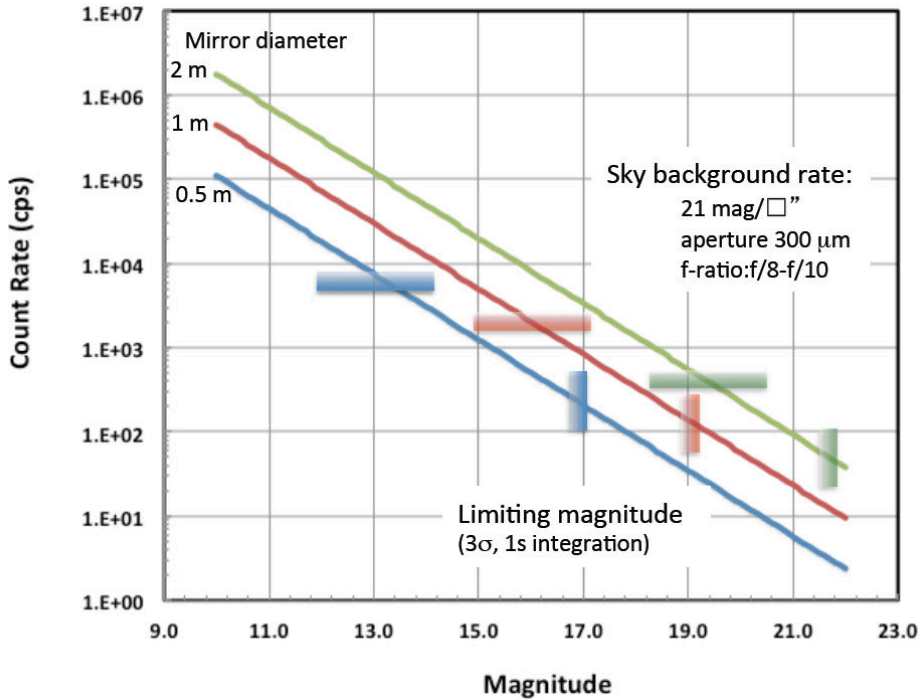


Figure 1. Typical count rates for a SPAD detector with $\sim 70\%$ maximum quantum efficiency at 680 nm ($> 35\%$ in the wavelength range 450-900 nm). The estimates are based on photometric calibrations of the OPTIMA detector at the 1.3m telescope of the Skinakas Observatory. Since the unfiltered SPAD response (450-900nm) does not correspond to a traditional astronomical filter, the magnitude (R, V, or I) can only be estimated roughly. The horizontal bars indicate the sky background level in the aperture ($S/N \sim 1$) and the vertical bars the limiting magnitude that can be detected in a one second time interval.

neutron stars, or black holes were detected with ground and space based instrumentation. While the large radio telescopes perform flux measurements for fast photometry, higher energy photons, roughly above the optical band, can be detected and time-tagged individually or in short integration time bins. Photon counting or fast imaging are therefore the techniques of choice for astronomy in the optical, X-ray, and gamma-ray bands.

In the optical band the first very fast photometers were based on photomultiplier tubes (PMT). The principle of converting a photon into a detectable electronic signal using the photo-effect in a thin, transparent photocathode was also employed in image intensifiers and multi-anode microchannel array (MAMA) detectors. Basic drawbacks of these systems are the low quantum effi-

ciency ($\sim 20-30\%$) and a rather narrow spectral response at short wavelengths. A positive characteristic is the low dark noise of these devices that can be obtained without or minimal cooling. Photon signals with a timing accuracy of a few nanoseconds can be achieved with PMTs.

The development of solid state photon detectors, in the form of individual photon diodes, their later variant as avalanche photo diodes (APD), and as CCD imaging devices, improved the quantum efficiency to values beyond 80%. The broad spectral response contributed also to the overall efficiency of solid state detectors. Thermal noise in semiconductor devices at room temperatures would however create unacceptable system noise levels and cooling is required. APDs and compact CCD cameras can be operated with thermoelectric cooling around 220-240K. Full astronomical CCDs are usually cooled with liquid nitrogen (160K) or electric cryocoolers. Single photon APD detectors (SPAD) can record signals with an accuracy of a few picoseconds. Frame transfer CCDs with a stage for electron multiplication (EM-CCDs) can now be read out at rates of several 10 Hz (full frame) or in small window mode up to a kHz.

Experimental photon calorimeters, i.e. devices where the heat deposited by individual optical or infrared photons is detected and measured, are based on quantum effects in cryogenic detectors with temperatures below 1K. Transition edge sensors (TES) use the sharp transition between normal and superconducting states. Small arrays have been developed (Romani et al., 2008) and prototypes were used, e.g. in the observation of the Crab pulsar (Romani et al., 2001). Superconducting tunnel junction detectors, based on the Josephson effect, were developed in small arrays in the S-CAM instrument (Verhoeve et al., 2006) and used for test measurements on telescopes. The newest generation cryogenic HTRA instrument is based on Microwave Kinetic Inductance Detectors (MKIDs) which enable simultaneous time- and energy-tagging of single photons (Mazin et al., 2013)

In the following short sections we present currently active HTRA instruments. Then we describe in more detail the photon counting instrument OPTIMA developed at the MPE. OPTIMA shares many typical components with other current photon counters (APD detectors, precise time tagging of single photons) and is an instrument that was developed and used over the last 15 years on telescopes with mirror sizes ranging from 1.3m to 3.5m.

3.1. 2-D fast imaging cameras

3.1.1. ULTRACAM

ULTRACAM is a portable CCD camera system for high-speed astrophysics (Dhillon et al. 2007). Optics with dichroic beam splitter mirrors produce simultaneous images in three colors which are recorded in three frame transfer CCD cameras. The CCDs can be read out with frame rates up to 500 Hz. ULTRACAM has been used on the 4.2m WHT, La Palma, the NTT and VLT in La

Silla, Chile. A single beam version called ULTRASPEC has been installed at the new Thai National Observatory 2.5m telescope and takes observations since November 2013.

3.1.2. ARCONS

The ARray Camera for Optical to Near-IR Spectrophotometry (ARCONS) is a new 2-D camera based on Microwave Kinetic Inductance Detectors (MKID), which are operated at cryogenic temperatures. ARCONS has been used at the Palomar 200" telescope, where it observed the Crab pulsar simultaneously with radio measurements from the Green Bank Telescope (Strader et al., 2013). This camera affords not only a field of view with 46x44 pixels but also 'energy' resolution for every detected photon.

3.2. Photon counting through apertures

The cameras described in this section are small portable devices and were used successfully at several observatories.

3.2.1. GASP

The Galway Astronomical Stokes Polarimeter is a fast, full Stokes, astronomical imaging polarimeter. Its construction allows to measure all four elements of the Stokes vector (I, Q, U, V) simultaneously over a broad wavelength range of 400-800 nm. Measuring linear and circular polarization with the time resolution of the order of microseconds makes GASP a unique astronomical instrument (Kyne et al. 2010).

3.2.2. IquEYE and AquEYE

These ultra-high-speed photometers are capable of tagging the arrival time of each photon with a resolution and accuracy of 50 picoseconds, for hours of continuous acquisition, and with a dynamic range of more than 6 orders of magnitude. The detector has four single photo avalanche diodes (SPADS) each illuminated by a beam reflected from a pyramid. Each beam can be filtered in bands of different color (Barbieri et al. 2009, 2012, Naletto et al., 2009). In recent observations of the Crab pulsar AquEYE demonstrated timing of the optical pulses with a resolution on the sub- μ s level (Germanà et al., 2012).

3.3. The OPTIMA photometer

The optical timing analyzer OPTIMA, in its previous configurations, has been described in Kanbach et al (2003, 2008). The principle of OPTIMA is based on time-tagging photons that are recorded through apertures located in the focal plane of a telescope.

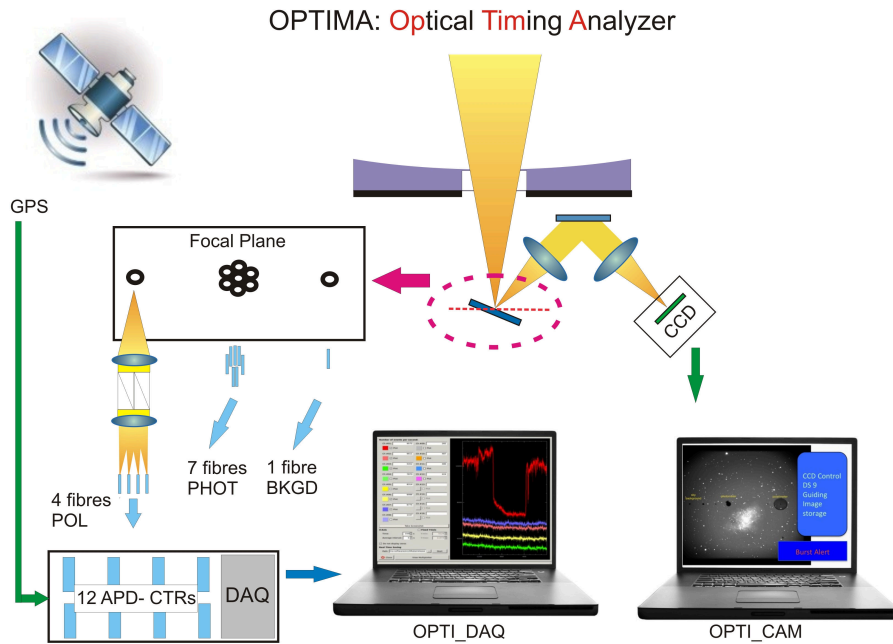


Figure 2. Schematic of the OPTIMA detector and its modes of operation: in the focal plane of a telescope an inclined mirror (in the dashed red ellipse) reflects the image of stars and targets to a CCD camera which is viewed online on the OPTI_CAM display (in the example an image of the Crab nebula is shown). Embedded in the focal plane mirror are optical fibres (one for the sky background and a hexagonal filled bundle for the target and its close environment) and an aperture for the polarimetry optics. The layout of apertures is shown left of the red ellipse. Using the OPTI_CAM imaging, where the photometry or polarimetry apertures are visible, targets can be positioned for the chosen mode and single photons are processed and recorded through the fibre coupled APD counters and time-tagging electronics. A quick-look display of rates is provided on the OPTI_DAQ computer and the photon lists are stored in FITS files for an off-line analysis.

The apertures are realized by optical fibers or a stop (diaphragm), which forms the entrance aperture of the twin Wollaston polarization optics. At the same time the environment of the apertures must be imaged to guide the acquisition of targets. This is realized by having the apertures embedded in a slanted mirror that reflects an image into a CCD camera. Series of continuous short ($\sim 10s$) CCD exposures of field stars are used to control the fine pointing and guidance of the telescope and analyzed to provide the status of atmospheric transparency and seeing conditions during a photon counting observation. Figure 2 shows a schematic of OPTIMA with details of the focal plane: a hexagonal

bundle of apertures for photometry, a single pin hole aperture for polarimetry with Wollaston optics, and an offset sky background aperture.

4. Selected results from OPTIMA observations at small telescopes

OPTIMA observations have been carried out at various observatories since the year 2000. Most time was spent at the 1.3m telescope of the Skinakas Observatory in cooperation with the University of Crete, Heraklion. OPTIMA followed a long-term program to detect and measure gamma-ray burst afterglows in their very early stages. Correlations between X-ray and optical emissions of suspected black hole and neutron star binary systems, and the optical emission from cataclysmic variables were also measured. In the following sections we summarize some of the notable results from Skinakas, and a very precise measurement of the optical polarization of the Crab pulsar obtained at the 2.5m telescope at the Nordic Optical Telescope, La Palma, Spain.

4.1. Correlated fast X-ray and optical variability in the black-hole candidate XTE J1118+480 (Kanbach et al., 2001)

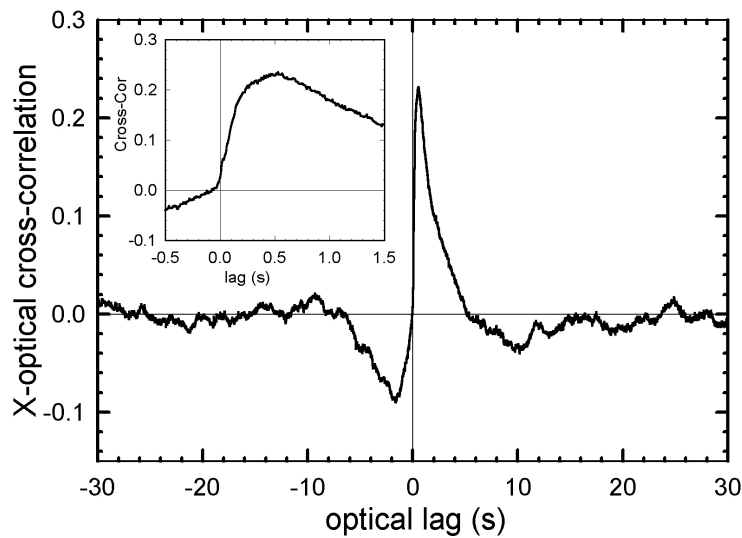


Figure 3. Cross-correlation of the X-ray and optical time series of XTE J1118+480 (KV UMa), showing the onset of an optical response within 30 ms after an outburst detected in X-rays. Positive lag corresponds to delay of optical emission.

Using simultaneous high-time-resolution X-ray (RXTE) and optical (OPTIMA) observations of the transient source XTE J1118+480 (a.k.a. KV UMa), we discovered strong and puzzling correlations between the emissions in these two bands. The optical emission rises suddenly, within 30 ms, following an increase in the X-ray output. We also observe a dip in the optical intensity about 2 s in advance of the X-rays. This result is not easy to understand within the simplest model where the optical emission is generated by reprocessed X-rays from an accretion disk. The data are more consistent with an earlier suggestion that the optical light is cyclo-synchrotron emission that originates in a region about 20,000 km from the black hole. We therefore proposed that the observed X-ray vs. optical time dependence is evidence for a relatively slow (0.1c), magnetically controlled outflow, where shocks from the central engine (X-rays) lead to optical emissions with the observed time delays.

4.2. Very fast optical flaring from a possible new Galactic magnetar (Stefanescu et al., 2008)

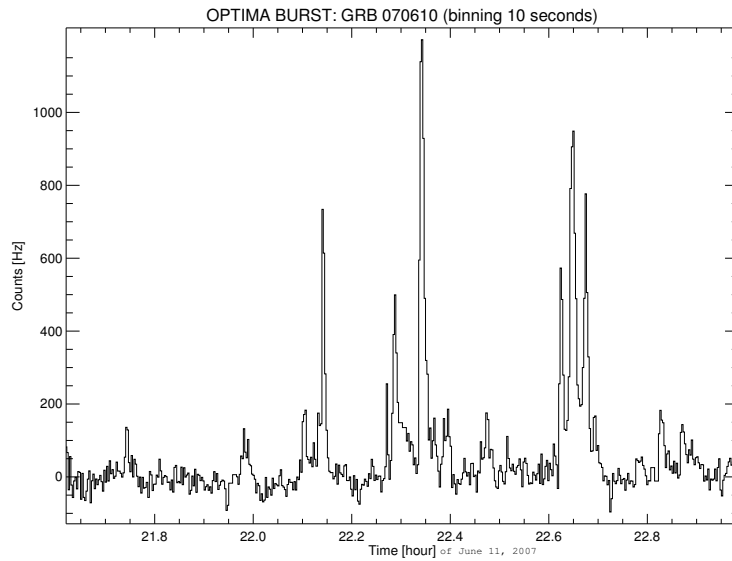


Figure 4. Fast optical flaring observed from SWIFT J1955+26 with OPTIMA on the 1.3m telescope of the Skinakas Observatory. This source was first detected with Swift in hard X-rays as a typical gamma-ray burst (GRB070610), but quick follow-up observations with optical cameras revealed the flaring and suggest that this source is likely to be a highly magnetized neutron star (magnetar) operating in the optical range.

Highly luminous rapid flares are characteristic of processes around compact objects like white dwarfs, neutron stars and black holes. In the high-energy regime of X-rays and gamma-rays, outbursts with variabilities on timescales of seconds or less are routinely observed, for example in gamma-ray bursts or soft gamma-ray repeaters. At optical wavelengths, flaring activity on such timescales had not been observed before. This is mostly due to the fact that outbursts with strong, fast flaring are usually discovered in the high-energy regime; most optical follow-up observations of such transients use instruments with integration times exceeding tens of seconds, which are therefore unable to resolve fast variability. With OPTIMA we discovered extremely bright and rapid optical flaring in the Galactic transient SWIFT J195509.6+261406. Figure 3 displays a sample of the light-curve during the second night after the initial detection. This kind of activity persisted only for a few days. The optical light curves are phenomenologically similar to high-energy light curves of soft gamma-ray repeaters and anomalous X-ray pulsars, which are thought to be neutron stars with extremely high magnetic fields (magnetars). This suggests that similar processes are in operation, but with strong emission in the optical, unlike in the case of other known magnetars.

4.3. Optical polarisation of the Crab pulsar: precision measurements and comparison to the radio emission (Słowikowska et al., 2009)

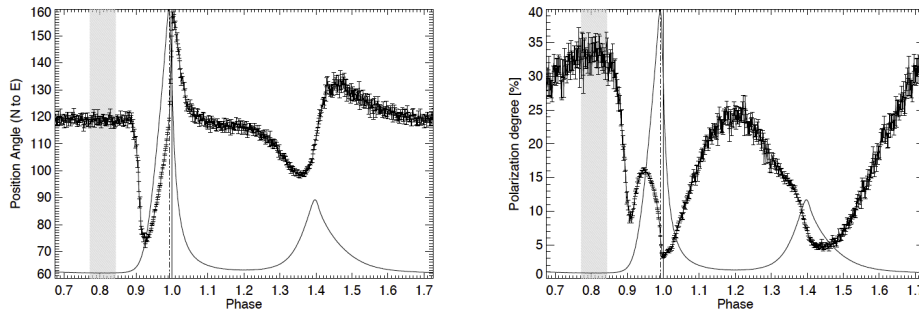


Figure 5. Linear optical polarization of the Crab pulsar: the position angle (PA, left panel) and the degree of polarization (PD, right panel) are shown as a function of the rotational phase of the pulsar. The PA changes are aligned with the main peak maximum of the optical light (vertical dot-dashed line), but also with the zero phase, i.e. with the MP radio phase (vertical solid line). The PD minimum is reached at the radio phase (vertical solid line), and not at the phase of the optical maximum (vertical dot-dashed line). For both panels a bit more than one rotation is shown for clarity. The optical pulse profile (solid line) and DC phase range (shaded region in the phase range 0.78-0.84) are also indicated.

The linear polarization of the Crab pulsar and its close environment was derived from OPTIMA observations at the 2.56-m Nordic Optical Telescope on La Palma. Time resolution as short as $11 \mu\text{s}$, which corresponds to a phase interval of $1/3000$ of the pulsar rotation, and high statistics allow the derivation of polarization details never achieved before (Fig. 5). The degree of optical polarization and the position angle correlate in surprising details with the light curves at optical wavelengths and at radio frequencies of 610 and 1400 MHz. Our observations also show that there exists a subtle connection between presumed non-coherent (optical) and coherent (radio) emissions: in the Crab main pulse the minimum of the optical polarization occurs at the phase of maximum radio emission and a strongly polarized optical component is observed at the phase of the low frequency radio precursor. These findings support previously detected correlations between the optical peak intensity and the occurrence of giant radio pulses in the Crab. Recent polarimetric imaging of the Crab pulsar and inner nebula with HST (Moran et al., 2013) confirmed essential results of the OPTIMA polarization measurement.

5. Conclusions

High time resolution instruments based on fast readout CCDs (resolution 1-2 ms) and SPADs with single photon time tagging with accuracy down to 50 picoseconds have been successfully used to detect rapidly changing astronomical sources such as optical pulsars, cataclysmic variables, including polars and intermediate polars, black hole binaries, and very fast flares from the first optical magnetar. These instruments therefore provide unique data to study the most compact stellar objects and reveal their spatial, spectral, and temporal properties.

References

- Barbieri, C., Naletto, G., Capraro, I., et al.: 2009, in *Photon Counting Applications, Quantum Optics, and Quantum Information Transfer and Processing II*, eds.: Prochazka, I., Dusek, M. and Sobolewski, R., SPIE conference series, Prague, vol. 7355
- Barbieri, C., Naletto, G., Zampieri, L., et al.: 2012, in *New Horizons in Time-Domain Astronomy*, eds.: R.E.M. Griffin, R.J. Hanisch and R. Seaman, IAU Symposium No. 285, Oxford, UK, 280
- Dhillon, V. S., Marsh, T. R., Stevenson, M. J., Atkinson, D. C., Kerry, P., Peacocke, P. T., Vick, A. J. A., Beard, S. M., Ives, D. J., Lunney, D. W., McLay, S. A., Tierney, C. J., Kelly, J., Littlefair, S. P., Nicholson, R., Pashley, R., Harlaftis, E. T., O'Brien, K.: 2007, *Mon. Not. R. Astron. Soc.* **378**, 825
- Germanà, C., Zampieri, L., Barbieri, C., Naletto, G., et al.: 2012, *Astron. Astrophys.* **548**, 47

- Kanbach, G., Kellner, S., Schrey, F., Steinle, H., Straubmeier, C., and Spruit, H. C.: 2003, in *Instrument Design and Performance for Optical/Infrared Ground-based Telescopes*, eds.: M. Iye and A. F. M. Moorwood, SPIE conference series vol. 4841, Waikoloa, USA, 82
- Kanbach, G., Stefanescu, A., Duscha, S., Mühlegger, M., Schrey, F., Steinle, H., Słowikowska, A., and Spruit, H. : 2008, *Astrophys. Space Sci. Library* **351**, 153
- Kanbach, G., Straubmeier, C., Spruit, H. C., Belloni, T.: 2001, *Nature* **414**, 180
- Kyne, G., Sheehan, B., Collins, P., Redfern, M., Shearer, A.: 2010, *EPJWC* **5**, 5003
- Mazin, B.A. et al.: 2013, *arXiv:1306.4674* ,
- Moran, P., Shearer, A., Mignani, R.P., Słowikowska, A., De Luca, A., Gouiffes, C., Laurent, P.: 2013, *Mon. Not. R. Astron. Soc.* **433**, 2564
- Naletto, G., Barbieri, C., Occhipinti, T., Capraro, I., et al.: 2009, *Astron. Astrophys.* **508**, 531
- Romani, R.W. et al.: 2001, *Astrophys. J.* **563**, 221
- Romani, R.W. et al.: 2008, *Astrophys. Space Sci. Lib* **351**, 311
- Słowikowska, A., Kanbach, G., Kramer, M., Stefanescu, A.: 2009, *Mon. Not. R. Astron. Soc.* **397**, 103
- Słowikowska, A., Goździewski, K., Nasiroglu, I., Kanbach, G., Rau, A., Krzeszowski, K.: 2013, in *18th European White Dwarf Workshop*, eds.: Krzesinski, J. , Stachowski, G. , P. Moskalik, P. and Bajan, K., ASP Vol. 469, Kraków, Poland, 363
- Stefanescu, A., Kanbach, G., Słowikowska, A., Greiner, J., McBreen, S., Sala, G.: 2008, *Nature* **455**, 503
- Strader, M.J. et al., 2013, arXiv:1309.3270v1
- Verhoeff, P. et al.: 2006, *Nucl. Instr. Meth. A* **559**, 598